Check for updates

Research Article

INTERNATIONAL JOURNAL OF ADVANCED ROBOTIC SYSTEMS

International Journal of Advanced Robotic Systems
January-February 2018: 1–8
© The Author(s) 2018
DOI: 10.1177/1729881418759106
journals.sagepub.com/home/arx
SAGE

Kinematic reliability and sensitivity analysis of the modified Delta parallel mechanism

Dongtao Xu

Abstract

In order to improve the kinematic reliability, it is crucial to find out the influence of each error source on the kinematic reliability of the mechanism. Reliability sensitivity analysis is used to find the changing rate in the probability of reliability in relation to the changes in distribution parameters. Based on the structural response surface function method, the functional relation between the kinematic reliability of a modified Delta parallel mechanism and the original input-error vectors is described using the quadratic function with cross terms. Moreover, the partial derivatives of the functional relation with respect to the means and variances of the original input errors are derived, which can efficiently evaluate kinematic reliability sensitivity of the mechanism. The advantages of this method are as follows: First, the response surface function, which can be easily set up by the position-error model of the mechanism, is convenient for calculating the variance, partial derivative, and reliability sensitivity. Second, in this case (unlike in the traditional error-mapping model), although the input-error values are unknown, pseudorandom variables used as random input-error sources can be generated by MATLAB software. Furthermore, the kinematic reliability of the mechanism can be assessed using the Monte Carlo method.

Keywords

Parallel mechanism, position and pose error, Monte Carlo method, kinematic reliability, reliability sensitivity

Date received: 5 November 2016; accepted: 20 January 2018

Topic: Robot Manipulation and Control
Topic Editor: Andrey V Savkin
Associate Editor: Alexander Pogromsky

Introduction

The Delta parallel mechanism was presented by Clavel[1] in 1988, as a high-speed parallel mechanism with three degrees of freedom (3-DOF). Currently, it is one of the most successful parallel mechanisms for commercial applications. However, it has the drawback of possessing several spherical joints, which are difficult to assemble and whose accuracy is difficult to guarantee. Tsai[2–4] invented a modified 3-DOF Delta parallel mechanism. Its most important properties are that all the kinematic joints are rotational joints and that it provides large workspace, high stiffness, low inertia, and large payload capacity.

Kinematic reliability is defined as the probability that the end effector position and orientation fall within a specified range of the desired location. Because of geometric errors in the components of the mechanism, as well as the position and pose errors of the joints, the end effector position of the mechanism will deviate from the ideal kinematic trajectory, thereby reducing the mechanism's kinematic accuracy.[5,6] Therefore, it is particularly important to determine whether the mechanism can accurately complete the specified motion by analyzing the kinematic reliability of

School of Mechanical Engineering & Automation, University of Science and Technology Liaoning, Anshan, Liaoning, China

Corresponding author:
Dongtao Xu, School of Mechanical Engineering & Automation, University of Science and Technology Liaoning, 185 Qianshan Zhong Road, Anshan, Liaoning 114051, China.
Email: as_xudongtao@163.com

Creative Commons CC BY: This article is distributed under the terms of the Creative Commons Attribution 4.0 License (http://www.creativecommons.org/licenses/by/4.0/) which permits any use, reproduction and distribution of the work without further permission provided the original work is attributed as specified on the SAGE and Open Access pages (https://us.sagepub.com/en-us/nam/open-access-at-sage).

this mechanism. The degree of influence of the errors on this kinematic reliability can be analyzed by means of kinematic reliability sensitivity analysis.[7–16] At present, studies on reliability sensitivity analysis mainly focus on the structural system of the mechanism. Reliability sensitivity analysis research on the kinematic system of the mechanism is limited, and breakthroughs have been scarce.[17,18]

This study aims to establish a kinematic-error model and analyze the kinematic reliability and reliability sensitivity of the modified Delta parallel mechanism, thus providing theoretical support for the design of such high-precision mechanisms.

Descriptions of the modified Delta parallel mechanism

The modified Delta parallel mechanism is shown in Figure 1.

The mechanism comprises a moving platform connected to a fixed platform by three parallel kinematic chains. Each chain contains a rotational joint activated by actuators on the fixed platform. The motion is transmitted to the moving platform through parallelograms formed by follower links and rotational joints, as shown in Figure 2.

The end effector of the mechanism is installed at the center of the moving platform; its coordinates are expressed as $[x, y, z]$. The rotational joints at points B_i and D_i (i =1, 2, 3) are placed in accordance with the equilateral triangle on the fixed and moving platforms.

The global coordinate system O-xyz is located at the center (point O) of the fixed platform. The xz plane coincides with the plane of the fixed platform, and the x-axis points to the center of the joint at point B_1 and the y-axis points vertically upward, as shown in Figure 3.

The reference coordinate system, A_i-$x_iy_iz_i$ ($i = 1, 2, 3$), is obtained when O-xyz revolves by an angle β_i ($i = 1, 2, 3$) around the y-axis, where β_i is 0°, 120°, or 240°, respectively.

The body-fitted coordinate system B_i-$x_iy_iz_i$, C_i-$x_iy_iz_i$, and D_i-$x_iy_iz_i$ are located at points B_i, C_i, and D_i, respectively. Their z_i-axes coincide with the axes of the joints B_i, C_i, and D_i, and their y_i-axes point vertically upward.

The body-fitted coordinate system of the moving platform is given by P-$x_iy_iz_i$, whose x_iz_i plane coincides with that of the moving platform and whose x_i-axis points to the center of joint D_1 and the y_i-axis points vertically upward. The reference coordinate system, F_i-$x_iy_iz_i$ ($i = 1, 2, 3$), is obtained when P-$x_iy_iz_i$ revolves β_i along the y_i-axis.

Kinematic-error model of the mechanism

According to Figure 3, a closed loop equation can be written for each chain

$$\boldsymbol{OP} = \boldsymbol{OB}_i + \boldsymbol{B}_i\boldsymbol{C}_i + \boldsymbol{C}_i\boldsymbol{C}_{ij} + \boldsymbol{C}_{ij}\boldsymbol{D}_{ij} + \boldsymbol{D}_{ij}\boldsymbol{D}_i - \boldsymbol{P}\boldsymbol{D}_i \quad (i = 1-3; j = 1-2) \tag{1}$$

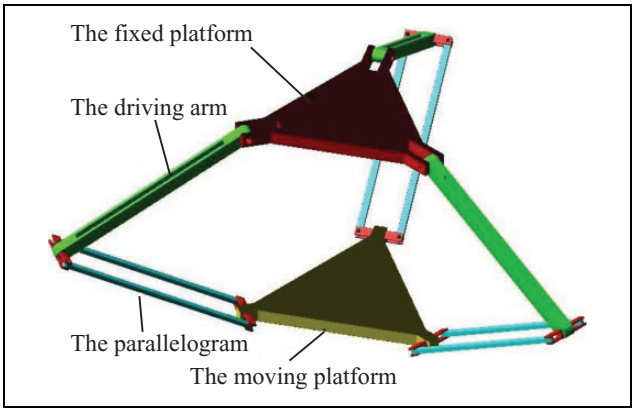


Figure 1. Modified Delta mechanism.

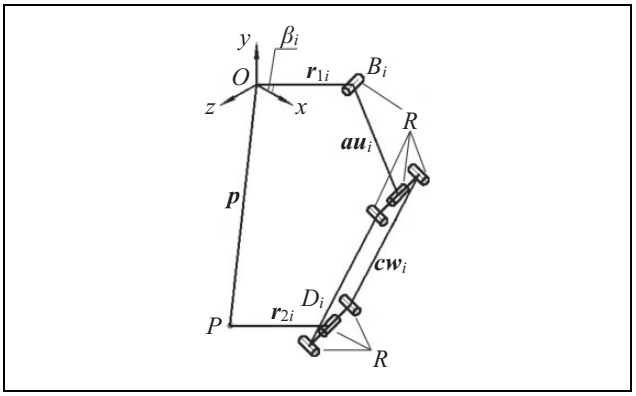


Figure 2. Descriptions of the kinematic chain.

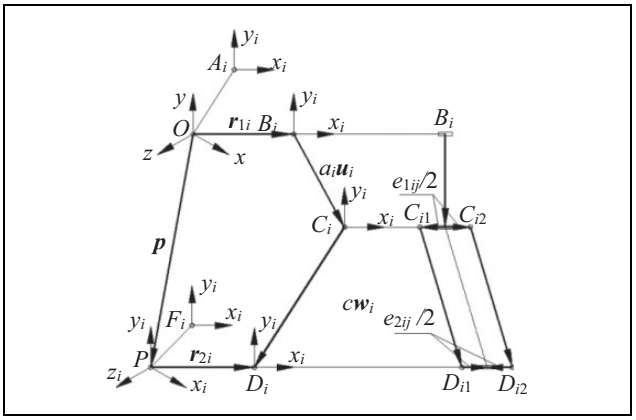


Figure 3. Coordinate system of the kinematic chain.

Rewriting equation (1) in the O-xyz coordinate frame leads to

$$\boldsymbol{P} = {}^{o}\boldsymbol{R}_{ai}\left(\boldsymbol{r}_{1i} + {}^{ai}\boldsymbol{R}_{bi}\left(a_i\boldsymbol{u}_i + (-1)^{j}\,{}^{bi}\boldsymbol{R}_{ci}\,{}^{e}{}_{1ij}/_{2}\boldsymbol{E}_2\right)\right) + c\boldsymbol{w}_i - {}^{o}\boldsymbol{R}_{fi}\left(\boldsymbol{r}_{2i} + (-1)^{j}\,{}^{fi}\boldsymbol{R}_{di}\,{}^{e}{}_{2ij}/_{2}\boldsymbol{E}_2\right) \quad (i = 1-3; j = 1-2) \tag{2}$$

where $\boldsymbol{E}_2 = (0, 0, 1)^{\mathrm{T}}$ and P is the position vector of the end effector.

Under small perturbations, the position of the end effector can be expressed as

$$\begin{aligned}\boldsymbol{P} + \Delta\boldsymbol{X} = {}^{o}\boldsymbol{R}_{ai}(\boldsymbol{r}_{1i} + \Delta\boldsymbol{r}_{1i}) + (c\boldsymbol{w}_i + \Delta c_{ij}\boldsymbol{w}_i + c\Delta\boldsymbol{w}_i) \\ -\mathrm{T}^{p}\boldsymbol{R}_{fi}\left(\boldsymbol{r}_{2i} + \Delta\boldsymbol{r}_{2i} + (-1)^{j}({}^{e_{1ij}}/_{2} + \Delta e_{2ij})\Xi\boldsymbol{E}_2\right) \\ +{}^{o}\boldsymbol{R}_{ai}\Psi\left((a_i\boldsymbol{u}_i + \Delta a_i\boldsymbol{u}_i) + (-1)^{j}({}^{e_{2ij}}/_{2} + \Delta e_{1ij})\Xi\boldsymbol{E}_2\right) \\ (i = 1-3; j = 1-2)\end{aligned} \tag{3}$$

where $\boldsymbol{E}_1$ is a 3×3 unit matrix, $T = (\boldsymbol{E}_1 + \boldsymbol{\theta}\times)$, $\Xi = (\boldsymbol{E}_1 + \boldsymbol{\theta}_{Ci}\times)$, $\Psi = (\boldsymbol{E}_1 + \boldsymbol{\theta}_{Bi}\times)$.

To obtain the position-error vectors $\Delta\boldsymbol{X}$ of the end effector, the following is done. Substituting $\boldsymbol{P}$ from equation (2) into equation (3) and simplifying, yields

$$\begin{aligned}\Delta\boldsymbol{X} = {}^{o}\boldsymbol{R}_{ai}\Lambda + \Delta c_{ij}\boldsymbol{w}_i + c\Delta\boldsymbol{w}_i - \mathrm{T}^{p}\boldsymbol{R}_{fi}\left(\boldsymbol{r}_2 + (-1)^{j}\,{}^{e_{1ij}}/_{2}\boldsymbol{E}_2\right) \\ -{}^{p}\boldsymbol{R}_{fi}\left(\Delta\boldsymbol{r}_{2i} + \Phi\left((-1)^{j}\,{}^{e_{1ij}}/_{2}\boldsymbol{E}_2\right) + \left((-1)^{j}\Delta e_{2ij}\boldsymbol{E}_2\right)\right) \\ (i = 1-3; j = 1-2)\end{aligned} \tag{4}$$

where $\Phi = (\boldsymbol{E}_1 + \boldsymbol{\theta}_{Di}\times)$ and

$$\begin{aligned}\Lambda = \Delta\boldsymbol{r}_{1i} + \Psi\left(a_i\boldsymbol{u}_i + (-1)^{j}\,{}^{e_{1ij}}/_{2}\boldsymbol{E}_2\right) + \Delta a_i\boldsymbol{u}_i \\ +\Xi\left((-1)^{j}\,{}^{e_{1ij}}/_{2}\boldsymbol{E}_2\right) + (-1)^{j}\Delta e_{1ij}\boldsymbol{E}_2\end{aligned}.$$

To eliminate the unit pose-error vector of the follower link, we multiply both sides of equation (4) by $\boldsymbol{w}_i^{\mathrm{T}}$ and simplify, which yields

$$\begin{aligned}\boldsymbol{w}_i^{\mathrm{T}}\Delta\boldsymbol{X} = \boldsymbol{w}_i^{\mathrm{T}}\,{}^{o}\boldsymbol{R}_{ai}\Delta\boldsymbol{k}_i + a_i({}^{o}\boldsymbol{R}_{ai}\boldsymbol{u}_i \times \boldsymbol{w}_i)^{\mathrm{T}}\,{}^{o}\boldsymbol{R}_{ai}\boldsymbol{\theta}_{Bi} + \Delta c_{ij} \\ + (-1)^{j}\left({}^{e_{1ij}}/_{2}({}^{o}\boldsymbol{R}_{ai}\boldsymbol{E}_2 \times \boldsymbol{w}_i)^{\mathrm{T}}\,{}^{o}\boldsymbol{R}_{ai}\boldsymbol{\theta}_i + \Delta e_{1ij}/_{2}\boldsymbol{w}_i^{\mathrm{T}}\,{}^{o}\boldsymbol{R}_{ai}\boldsymbol{E}_2\right) \\ + \boldsymbol{w}_i^{\mathrm{T}}\,{}^{o}\boldsymbol{R}_{ai}\boldsymbol{u}_i\Delta a_i - \left({}^{p}\boldsymbol{R}_{fi}\left(\boldsymbol{r}_{2i} + (-1)^{j}\,{}^{e_{2ij}}/_{2}\boldsymbol{E}_2\right) \times \boldsymbol{w}_i\right)^{\mathrm{T}}\boldsymbol{\theta} \\ (i = 1-3; j = 1-2)\end{aligned} \tag{5}$$

where $\Delta\boldsymbol{k}_i = \Delta\boldsymbol{r}_{1i} - \Delta\boldsymbol{r}_{2i}$ and $\boldsymbol{\theta}_i = \boldsymbol{\theta}_{Bi} + \boldsymbol{\theta}_{Ci} - \boldsymbol{\theta}_{Di.}$

Subtracting equation (5) at $j = 2$ from equation (5) at $j = 1$ leads to

$$\begin{aligned}e_{1ij}({}^{o}\boldsymbol{R}_{ai}\boldsymbol{E}_2 \times \boldsymbol{w}_i)^{\mathrm{T}}\boldsymbol{\theta} = \Delta c_{id} + \Delta e_{1ij}\boldsymbol{w}_i^{\mathrm{T}}\,{}^{o}\boldsymbol{R}_{ai}\boldsymbol{E}_2 \\ + e_{2ij}({}^{p}\boldsymbol{R}_{fi}\boldsymbol{E}_2 \times \boldsymbol{w}_i)^{\mathrm{T}}\,{}^{o}\boldsymbol{R}_{ai}\boldsymbol{\theta}_i \\ (i = 1-3)\end{aligned} \tag{6}$$

where $\Delta c_{id} = \Delta c_{i2} - \Delta c_{i1.}$

Simplifying equation (6), the pose-error mapping model of the mechanism can be constructed as

$$\boldsymbol{\theta} = \boldsymbol{J}_{\theta}\varepsilon_{\theta} \tag{7}$$

where $\boldsymbol{J}_{\theta} = \boldsymbol{A}^{-1}\boldsymbol{B}$, $\boldsymbol{A} = e_{1ij}[{}^{o}\boldsymbol{R}_{a1}\boldsymbol{E}_2 \times \boldsymbol{w}_1\ {}^{o}\boldsymbol{R}_{a2}\boldsymbol{E}_2 \times \boldsymbol{w}_2\ {}^{o}\boldsymbol{R}_{a3}\boldsymbol{E}_2 \times \boldsymbol{w}_3]^{\mathrm{T}}$, $\boldsymbol{B} = \mathrm{diag}[\boldsymbol{B}_i]^{\mathrm{T}}$, $\boldsymbol{B}_i = [1\ \boldsymbol{w}_i{}^{\mathrm{T}o}\boldsymbol{R}_{ai}\boldsymbol{E}_2\ e_{2ij}({}^{o}\boldsymbol{R}_{ai} \times \boldsymbol{w}_i)^{\mathrm{T}o}\boldsymbol{R}_{ai}]$, $\varepsilon_{\theta} = [\varepsilon_{\theta 1}^{\mathrm{T}}\ \varepsilon_{\theta 2}^{\mathrm{T}}\ \varepsilon_{\theta 3}^{\mathrm{T}}]^{\mathrm{T}}$, $\varepsilon_{\theta i}^{\mathrm{T}} = [\Delta c_{id}\ \Delta e_i\ \boldsymbol{\theta}_i{}^{\mathrm{T}}]^{\mathrm{T}}$, and $\Delta e_i = 2(\Delta e_{1ij} - \Delta e_{2ij})$.

Adding equation (5) at $j = 2$ and equation (5) at $j = 1$ leads to

$$\begin{aligned}\boldsymbol{w}_i^{\mathrm{T}}\Delta\boldsymbol{X} = \Delta c_{Pi} + \boldsymbol{w}_i^{\mathrm{T}}\,{}^{o}\boldsymbol{R}_{ai}\boldsymbol{u}_i\Delta a_i + \boldsymbol{w}_i^{\mathrm{T}}\,{}^{o}\boldsymbol{R}_{ai}\Delta\boldsymbol{k}_i \\ +a_i({}^{o}\boldsymbol{R}_{ai}\boldsymbol{u}_i \times \boldsymbol{w}_i)^{\mathrm{T}}\,{}^{o}\boldsymbol{R}_{ai}\boldsymbol{\theta}_{Bi} - ({}^{p}\boldsymbol{R}_{fi}\boldsymbol{r}_{2i} \times \boldsymbol{w}_i)^{\mathrm{T}}\boldsymbol{\theta} \\ (i = 1-3)\end{aligned} \tag{8}$$

where $\Delta c_{Pi} = (\Delta c_{i2} + \Delta c_{i1})/2$.

Substituting $\boldsymbol{\theta}$ in equation (7) into equation (8), the position-error mapping model of the mechanism can be constructed as

$$\Delta\boldsymbol{X} = \boldsymbol{J}_P\varepsilon = [\,\boldsymbol{J}_{PP} \quad \boldsymbol{J}_{PJ}\,]\begin{bmatrix}\varepsilon_{PP} \\ \varepsilon_{\theta}\end{bmatrix} \tag{9}$$

where $\boldsymbol{J}_{PP} = \boldsymbol{C}^{-1}\boldsymbol{D}$, $\boldsymbol{C} = [\boldsymbol{w}_1\ \boldsymbol{w}_2\ \boldsymbol{w}_3]^{\mathrm{T}}$, $\boldsymbol{D} = \mathrm{diag}[\boldsymbol{D}_i]^{\mathrm{T}}$, $\boldsymbol{D}_i = [1\ \boldsymbol{w}_i^{\mathrm{T}o}\boldsymbol{R}_{ai}\boldsymbol{u}_i\ \boldsymbol{w}_i^{\mathrm{T}o}\boldsymbol{R}_{ai}\ a({}^{o}\boldsymbol{R}_{ai}\boldsymbol{u}_i \times \boldsymbol{w}_i)^{\mathrm{T}o}\boldsymbol{R}_{ai}]$, $\boldsymbol{J}_{PJ} = \boldsymbol{C}^{-1}\boldsymbol{E}\boldsymbol{J}_{\theta}$, $\boldsymbol{E} = -[{}^{o}\boldsymbol{R}_{a1}\boldsymbol{r}_2 \times \boldsymbol{w}_1\ {}^{o}\boldsymbol{R}_{a2}\boldsymbol{r}_2 \times \boldsymbol{w}_2\ {}^{o}\boldsymbol{R}_{a3}\boldsymbol{r}_2 \times \boldsymbol{w}_3]^{\mathrm{T}}$, $\varepsilon_{PP} = [\varepsilon_{PP1}^{\mathrm{T}}\ \varepsilon_{PP2}^{\mathrm{T}}\ \varepsilon_{PP3}^{\mathrm{T}}]^{\mathrm{T}}$, $\varepsilon_{PPi} = [\Delta c_{iP}\ \Delta a_i\ \Delta\boldsymbol{k}_i{}^{\mathrm{T}}\ \boldsymbol{\theta}_{Bi}{}^{\mathrm{T}}]^{\mathrm{T}}$, and $\Delta\boldsymbol{k}_i = \Delta\boldsymbol{r}_{1i} - \Delta\boldsymbol{r}_{2i}$.

Equations (7) and (9) show that 21 geometric errors affect the position and pose precision of the end effector, 9 geometric errors only affect the position precision of the end effector.

Kinematic reliability analysis of the mechanism using the Monte Carlo method

The Monte Carlo method is a numerical calculation method used to find an approximate solution to technical engineering problems by generating random statistical sampling data using a computer.

The process of evaluating kinematic reliability using the Monte Carlo method is as follows:

The mean values of the geometric errors of all components and joints were obtained according to the upper- and lower-limit deviations of all geometric errors because the geometric errors of individual parts obey the normal distribution, so the error means μ_i and variance σ_i can be obtained.

The random-error parameters Δy_{ij} ($i = 1, 2 \ldots, m$, where m is the number of error sources; $j = 1, 2 \ldots, n$, where n is the number of generated samples) can be generated using the normrnd(μ_i, σ_i) function in MATLAB [version 6.5]. The kinematic errors of this mechanism can be obtained by substituting Δy_{ij} into equations (7) and (9). By repeating the above operation n times, n samples ΔX_i ($i = 1, 2 \ldots, n$) of the output kinematic error can be obtained. Keep count of

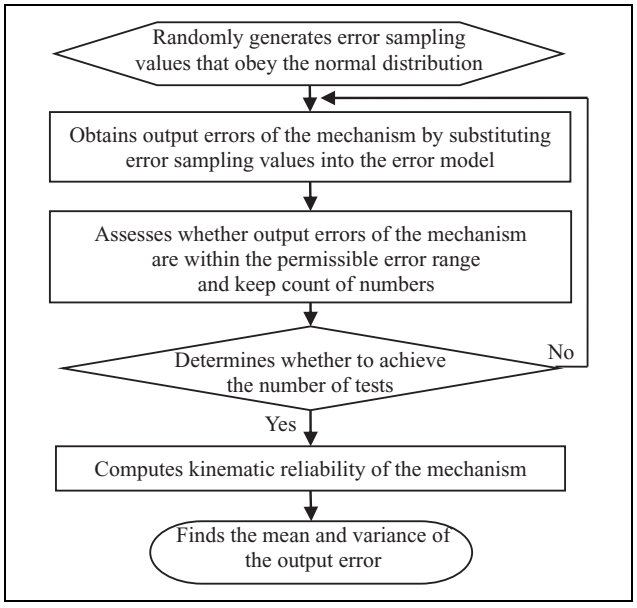


Figure 4. Flowchart of kinematic reliability analysis.

numbers ($s = s + 1$) if the output kinematic error is less than or equal to the permissible error ($\Delta X_i \leq \Delta$) before achieving the number of tests. According to the law of large numbers, the kinematic reliability of the mechanism is $R = s/n$. A flowchart of the reliability calculation is shown in Figure 4.

Reliability sensitivity analysis

The response surface function is based on the idea that when the output response is unknown, the relation between the output response and the input random parameter vector can be described by a quadratic function with a cross term.

By constructing the response surface function, the mapping relation between the random variables of the input errors and the position error of the mechanism can be established; namely, the functional relation between the position error of the mechanism, ΔX, and the input-error vector, $\boldsymbol{y} = (y_1, y_2, \ldots, y_n)$, can be described by a quadratic function containing the cross term, as shown below

$$\Delta X = C_0 + \sum_{i=1}^{n} C_i y_i + \sum_{i=1}^{n}\sum_{j=i}^{n} C_{ij} y_i y_j \quad (i = 1 \ldots n; j = i \ldots n) \tag{10}$$

where C_0, C_i, C_{ij} ($i = 1 \ldots n; j = i \ldots n$) are undetermined coefficients.

When the permissible error obeys the normal distribution, the limit state function of kinematic reliability is

$$G(X) = \Delta - \Delta X = \Delta - \left(C_0 + \sum_{i=1}^{n} C_i y_i + \sum_{i=1}^{n}\sum_{j=i}^{n} C_{ij} y_i y_j\right) \quad (i = 1 \ldots n; j = i \ldots n) \tag{11}$$

According to the Monte Carlo method, the mean and variance of the output position error of the mechanism can be obtained as

$$\begin{cases} \mu = \dfrac{1}{s}\displaystyle\sum_{i=1}^{s} \Delta X_i \\ \sigma^2 = \dfrac{1}{s-1}\displaystyle\sum_{i=1}^{s} (\Delta X_i - \mu)^2 \end{cases} \tag{12}$$

The reliability index is obtained as

$$\beta = \frac{\mu}{\sqrt{D}} \tag{13}$$

Because $G(X)$ follows a normal distribution, the kinematic reliability of the mechanism can also be expressed as

$$R = P(\Delta X < \Delta) = \Phi(\beta) \tag{14}$$

where $\Phi(\bullet)$ is the standard normal distribution function.

Differentiating equation (14) with respect to the mean matrix, μ_i, and the variance matrix, $\boldsymbol{D}_i$, of the random-parameter error, the kinematic reliability sensitivity is obtained

$$\frac{\partial R}{\partial \boldsymbol{\mu}_i^{\mathrm{T}}} = \frac{\partial R}{\partial \beta}\left(\frac{\partial \beta}{\partial \mu}\frac{\partial \mu}{\partial \boldsymbol{\mu}_i^{\mathrm{T}}} + \frac{\partial \beta}{\partial D}\frac{\partial D}{\partial \boldsymbol{\mu}_i^{\mathrm{T}}}\right) \quad (i = 1 \ldots n) \tag{15}$$

$$\frac{\partial R}{\partial \boldsymbol{D}_i^{\mathrm{T}}} = \frac{\partial R}{\partial \beta}\left(\frac{\partial \beta}{\partial \mu}\frac{\partial \mu}{\partial \boldsymbol{D}_i^{\mathrm{T}}} + \frac{\partial \beta}{\partial D}\frac{\partial D}{\partial \boldsymbol{D}_i^{\mathrm{T}}}\right) \quad (i = 1 \ldots n) \tag{16}$$

where $\frac{\partial R}{\partial \beta} = \Phi(\beta)$, $\frac{\partial \beta}{\partial \mu} = \frac{1}{\sqrt{D}}$, $\frac{\partial \beta}{\partial D} = -\frac{\mu}{2} D^{-3/2}$, $\frac{\partial \mu}{\partial \boldsymbol{\mu}_i^{\mathrm{T}}} = \left[\frac{\partial \mu}{\partial \mu_1}, \frac{\partial \mu}{\partial \mu_2}, \mathrm{K}, \frac{\partial \mu}{\partial \mu_n}\right]^{\mathrm{T}}$, $\frac{\partial \mu}{\partial \boldsymbol{D}_i^{\mathrm{T}}} = \left[\frac{\partial \mu}{\partial D_1}, \frac{\partial \mu}{\partial D_2}, \mathrm{K}, \frac{\partial \mu}{\partial D_n}\right]^{\mathrm{T}}$, $\frac{\partial D}{\partial \boldsymbol{\mu}_i^{\mathrm{T}}} = \left[\frac{\partial D}{\partial \mu_1}, \frac{\partial D}{\partial \mu_2}, \mathrm{K}, \frac{\partial D}{\partial \mu_n}\right]^{\mathrm{T}}$, and $\frac{\partial D}{\partial \boldsymbol{D}_i^{\mathrm{T}}} = \left[\frac{\partial D}{\partial D_1}, \frac{\partial D}{\partial D_2}, \mathrm{K}, \frac{\partial D}{\partial D_n}\right]^{\mathrm{T}}$.

Numerical example

The parameters of the mechanism are specified as follows: $a_i = c = 1000$ mm, $e_{1ij}/2 = 50$ mm, and $\boldsymbol{r}_{1i} = \boldsymbol{r}_{2i} = [500\ 0\ 0]^{\mathrm{T}}$ mm. The initial output position coordinate of the end effector is $[0\ 1000\ 0]^{\mathrm{T}}$ mm. The input angular accelerations of three driving arms are $0.5°/s^2$, $-0.5°/s^2$, and $1°/s^2$.

Numerical example of error analysis of the mechanism

The length errors of the driving arms are given as $\Delta a_1 = 0.5$ mm, $\Delta a_2 = -1$ mm, and $\Delta a_3 = -0.5$ mm, and other errors are ignored. The output position error, $\Delta \boldsymbol{X}$, of the mechanism is shown in Figure 5.

The length errors of follower links are given as $\Delta c_{21} = 0.5$ mm, $\Delta c_{22} = 0$ mm, $\Delta c_{21} = 0$ mm, $\Delta c_{22} = -0.5$ mm, $\Delta c_{31} = 1$ mm, and $\Delta c_{32} = -1$ mm, and other errors are ignored. $\Delta \boldsymbol{X}$ of the mechanism is shown in Figure 6.

The configuration-position-error vector of the joint at points B_i and D_i are given by $\Delta \boldsymbol{r}_{11} = [1\ 0.5\ -0.5]^{\mathrm{T}}$,

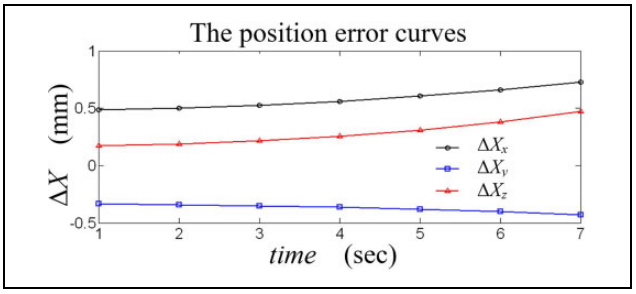


Figure 5. Effect of driving-arm-length error on output errors of the mechanism as a function of time.

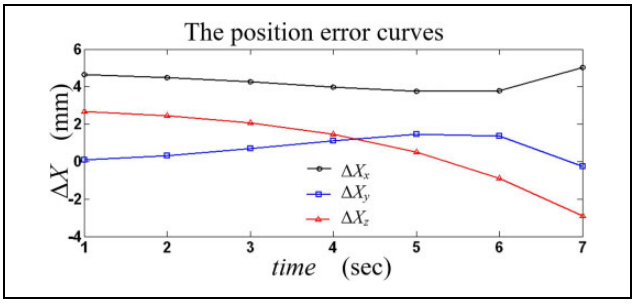


Figure 6. Effect of the follower link's length error on output errors of the mechanism as a function of time.

$\Delta \boldsymbol{r}_{21} = [-1\ -0.5\ 0.5]^{\mathrm{T}}$, $\Delta \boldsymbol{r}_{12} = [1\ 0.5\ -0.5]^{\mathrm{T}}$, $\Delta \boldsymbol{r}_{22} = [-1\ -0.5\ 0.5]^{\mathrm{T}}$, $\Delta \boldsymbol{r}_{13} = [1\ 0.5\ -0.5]^{\mathrm{T}}$, and $\Delta \boldsymbol{r}_{23} = [-1\ -0.5\ 0.5]^{\mathrm{T}}$, and other errors are ignored. $\Delta \boldsymbol{X}$ of the mechanism is shown in Figure 7.

The pose errors of the coordinate systems are given by B_i-$x_iy_iz_i$, C_i-$x_iy_iz_i$, and D_i-$x_iy_iz_i$: $\boldsymbol{\theta}_{Bi} = \boldsymbol{\theta}_{Ci} = \boldsymbol{\theta}_{Di} = [0.5*\mathrm{pi}/180\ 0.5*\mathrm{pi}/180\ 0]^{\mathrm{T}}$, and other errors are ignored. $\Delta \boldsymbol{X}$ of the mechanism is shown in Figure 8.

The length errors of the shafts C_iC_{ij} $(j = 1, 2)$ are given as $\Delta e_{111} = 0.5$, $\Delta e_{121} = -0.5$, $\Delta e_{112} = 0.5$, $\Delta e_{122} = -0.5$, $\Delta e_{113} = 0.5$, and $\Delta e_{123} = -0.5$, and other errors are ignored. $\Delta \boldsymbol{X}$ of the mechanism is shown in Figure 9.

The following conclusions are obtained from Figures 5 to 9.

The length errors of the driving arms have little influence on the position error of the mechanism. The effect of the follower links' length errors on the position error is larger than that of the driving arms. They affect both the position and pose accuracy of the mechanism when the lengths of two follower links differ. The length errors of shafts C_iC_{ij} have a great influence on the position error of the mechanism. This effect will gradually increase with the lateral movement of the end effector. These factors, including the configuration-position errors and the pose errors of the joints, seriously affect the mechanism's position and pose errors.

Numerical example of kinematic reliability analysis of the mechanism

The kinematic reliability of the mechanism can be analyzed using the Monte Carlo method when nominal dimensions

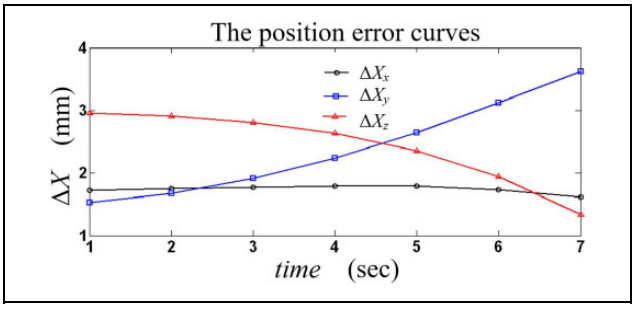


Figure 7. Effect of each chain's position on the mechanism's position errors.

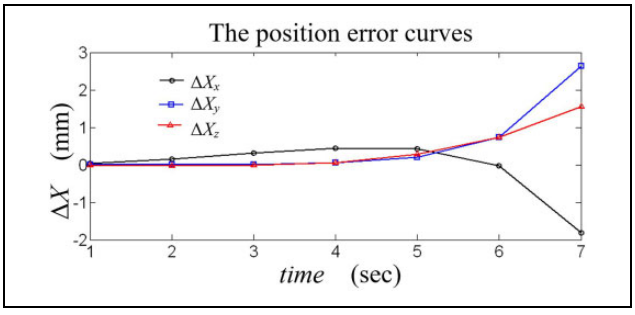


Figure 8. Effect of the components' attitude error on the mechanism's position errors.

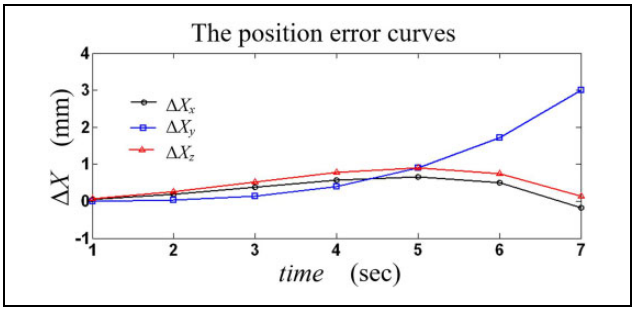


Figure 9. Effect of the connecting-shaft-length error on the mechanism's position errors.

and geometric tolerances of the parts are given, such as setting the lengths of the driving arms and follower links as $a_i = 1000 \pm 1$ mm and $c_i = 1000 \pm 1$ mm; the vector components of the configuration-position errors of the joints at B_i and D_i as $r_{1ix} = r_{2ix} = \pm 1$ mm and $r_{1iy} = r_{2iy} = r_{1iz} = r_{2iz} = \pm 0.5$ mm; the lengths of links C_iC_{ij} $(j = 1, 2)$ as $e_{1i} = e_{2i} = 100 \pm 0.5$ mm; and the vector components of the pose errors of the joints at points B_i, C_i, and D_i as $\theta_{Bix} = \theta_{Biy} = \pm 0.3°$, $\theta_{Cix} = \theta_{Ciy} = \pm 0.3°$, and $\theta_{Dix} = \theta_{Diy} = \pm 0.3°$. Three joints can rotate freely around the z-axis; therefore, the z components of pose errors are 0. The number of samples is $n = 400$.

When the mechanism has a 7-s motion and the maximum permissible limit of the position error of the mechanism is $\Delta = [5\ -5\ 8]^{\mathrm{T}}$, kinematic reliability is determined based on the Monte Carlo method, as shown in Table 1.

Table 1. Reliability calculation.

Time (s)	1	2	3	4	5	6	7
R (%)	100	100	99.75	99.00	98.75	94.00	72.50

According to the data in Table 1, we find that the kinematic reliability of the mechanism was better when its end effector was near the initial position. With the lateral movement of the end effector, the kinematic reliability of the mechanism gradually reduced. In particular, when a driving arm moves to a horizontal position, the kinematic reliability reaches its lowest value, which is only 72.50%; therefore, the position of the mechanism should not be listed as being in a reasonable working space.

The calculations of position reliability in Table 1 are consistent with the kinematic-error distribution in Figures 5 to 9. When the position error of the mechanism increases, the kinematic reliability of the mechanism decreases.

Numerical example of kinematic reliability sensitivity analysis of the mechanism

According to equation (10), the response surface function of the kinematic position error can be constructed as

$$\begin{aligned}\Delta \boldsymbol{X} = {} & C_1\delta c_{1P} + C_2\delta a_1 + C_3\delta \boldsymbol{k}_1{}^{\mathrm{T}} + C_4\boldsymbol{\theta}_{B1}^{\mathrm{T}} + C_5\delta c_{2P} \\ & + C_6\delta a_2 + C_7\delta \boldsymbol{k}_2{}^{\mathrm{T}} + C_8\boldsymbol{\theta}_{B2}^{\mathrm{T}} + C_9\delta c_{3P} + C_{10}\delta a_3 \\ & + C_{11}\delta k_3{}^{\mathrm{T}} + C_{12}\boldsymbol{\theta}_{B3}^{\mathrm{T}} + C_{13}\delta c_{1d} + C_{14}\delta e_1 + C_{15}\boldsymbol{\theta}_1^{\mathrm{T}} \\ & + C_{16}\delta c_{2d} + C_{17}\delta e_2 + C_{18}\boldsymbol{\theta}_2^{\mathrm{T}} + C_{19}\delta c_{3d} + C_{20}\delta e_3 \\ & + C_{21}\boldsymbol{\theta}_3^{\mathrm{T}}\end{aligned} \tag{17}$$

where $C_1 = J_{PP}$ (3,[1]), J_{PP} (3,[1]) represents the first column of the 3×24 matrix J_{PP}, $C_2 = J_{PP}$ (3,[2]), $C_3 = J_{PP}$ (3,[3,4,5]), J_{PP} (3,[3,4,5]) represents columns 3, 4, and 5 of the 3×24 matrix J_{PP}, $C_4 = J_{PP}$ (3,[6,7,8]), $C_5 = J_{PP}$ (3,[9]), $C_6 = J_{PP}$ (3,[10]), $C_7 = J_{PP}$ (3,[11,12,13]), $C_8 = J_{PP}$ (3,[14,15,16]), $C_9 = J_{PP}$ (3,[17]), $C_{10} = J_{PP}$ (3,[18]), $C_{11} = J_{PP}$ (3,[19,20,21]), $C_{12} = J_{PP}$ (3,[22,23,24]), $C_{13} = J_{PJ}$ (3,[1]), J_{PJ} represents a 3×15 matrix, $C_{14} = J_{PJ}$ (3,[2]), $C_{15} = J_{PJ}$ (3,[3,4,5]), $C_{16} = J_{PJ}$ (3,[6]), $C_{17} = J_{PJ}$ (3,[7]), $C_{18} = J_{PJ}$ (3,[8,9,10]), $C_{19} = J_{PJ}$ (3,[11]), $C_{20} = J_{PJ}$ (3,[12]), and $C_{21} = J_{PJ}$ (3,[13,14,15]).

If Δ is the maximum permissible limit of the position error of the mechanism, according to equation (11), the limit state function of the kinematic reliability can be obtained

$$\begin{aligned}G(\boldsymbol{X}) = \Delta - \Delta\boldsymbol{X} = {} & \Delta - C_0 - C_1\delta c_{1P} - C_2\delta a_1 - C_3\delta \boldsymbol{k}_1{}^{\mathrm{T}} \\ & - C_4\boldsymbol{\theta}_{B1}^{\mathrm{T}} - C_5\delta c_{2P} - C_6\delta a_2 - C_7\delta \boldsymbol{k}_2{}^{\mathrm{T}} - C_8\boldsymbol{\theta}_{B2}^{\mathrm{T}} - C_9\delta c_{3P} \\ & - C_{10}\delta a_3 - C_{11}\delta \boldsymbol{k}_3{}^{\mathrm{T}} - C_{12}\boldsymbol{\theta}_{B3}^{\mathrm{T}} - C_{13}\delta c_{1d} - C_{14}\delta e_1 - C_{15}\boldsymbol{\theta}_1^{\mathrm{T}} \\ & - C_{16}\delta c_{2d} - C_{17}\delta e_2 - C_{18}\boldsymbol{\theta}_2^{\mathrm{T}} - C_{19}\delta c_{3d} - C_{20}\delta e_3 - C_{21}\boldsymbol{\theta}_3^{\mathrm{T}}\end{aligned} \tag{18}$$

When the end effector of the mechanism reaches point P $(22.8851, -907.9187, 110.9301)^{\mathrm{T}}$ in the workspace, the mean and variance of the output kinematic-position error can be obtained as $\mu = [0.5847, -4.1119, 4.2196]$ and $\boldsymbol{D} = [11.0853, 1.5325, 10.0855]$, respectively, according to the Monte Carlo method. At this moment, the kinematic reliability sensitivities of the means and variances are shown in Tables 2 and 3 according to equations (15) and (16), respectively.

When the kinematic reliability sensitivity is 0, the reliability of the mechanism does not change with random errors. The magnitudes of the sensitivity's absolute value indicate the rate at which the reliability changes with random errors.

The results of kinematic reliability sensitivity analysis can be seen in Tables 2 and 3.

Reliability sensitivity data in Tables 2 and 3 are in good agreement with the position errors of the mechanism in Figures 5 to 9.

We can see from the kinematic reliability sensitivity analysis in Tables 2 and 3 that the mean of the pose-error

Table 2. Kinematic reliability sensitivity to the mean of each error component ($\times 10^{-3}$).

$\partial R/\partial \mu^{\mathrm{T}}$		δc_{iP}	δa_i	$\boldsymbol{\theta}_{Bi}$	δc_{id}	δe_i	$\boldsymbol{\theta}_i$
Rx	$i = 1$	−0.18	0.16	8.90	−0.18	−0.02	−8.45
	$i = 2$	0.10	−0.10	2.05	0.99	−0.04	34.87
	$i = 3$	0.09	−0.08	2.64	−0.74	0.06	−39.49
Ry	$i = 1$	−0.50	0.23	49.59	0.98	0.11	−85.40
	$i = 2$	−0.39	0.14	−11.49	−0.45	0.02	42.11
	$i = 3$	−0.55	0.29	−38.10	−0.51	0.04	43.18
Rz	$i = 1$	0.02	0.002	−13.70	0.89	0.09	0
	$i = 2$	0.19	−0.01	−151.01	−0.61	0.02	0
	$i = 3$	−0.14	0.01	110.55	−0.27	0.02	0

Table 3. Kinematic reliability sensitivity to the variance of each error component ($\times 10^{-3}$).

$\partial R/\partial D^{\mathrm{T}}$		δc_{iP}	δa_i	$\boldsymbol{\theta}_{Bi}$	δc_{id}	δe_i	$\boldsymbol{\theta}_i$
Rx	$i = 1$	0.01	−0.01	−0.23	0.01	0.01	0.22
	$i = 2$	−0.01	0.01	−0.05	−0.03	0.01	−0.92
	$i = 3$	−0.01	0.01	−0.07	0.02	−0.01	1.04
Ry	$i = 1$	−0.67	0.39	66.54	1.31	0.15	−114.57
	$i = 2$	−0.52	0.30	−15.43	−0.60	0.02	56.49
	$i = 3$	−0.73	0.43	−51.11	−0.69	0.05	57.93
Rz	$i = 1$	−0.01	0.01	2.87	−0.19	−0.02	0
	$i = 2$	−0.04	0.02	31.61	0.13	−0.01	0
	$i = 3$	0.03	−0.02	−23.14	0.06	−0.01	0

vectors, $\boldsymbol{\theta}_{Bi}$, and the composite-pose-error vectors, $\boldsymbol{\theta}_i$, have a larger influence on the kinematic reliability of the mechanism. In the z direction, the mean of $\boldsymbol{\theta}_{Bi}$ has the largest influence on the kinematic reliability, but the mean of $\boldsymbol{\theta}_i$ has no effect.

The variances of the pose-error vectors $\boldsymbol{\theta}_{Bi}$ and $\boldsymbol{\theta}_i$ have a larger influence on the kinematic reliability of the mechanism. In the y direction, the variances of $\boldsymbol{\theta}_i$ have the largest influence on the kinematic reliability. In the z direction, the variance of $\boldsymbol{\theta}_i$ has no effect on the kinematic reliability.

The influence of the pose errors of the joints on the kinematic reliability of the mechanism is much larger than that of the dimension errors of the components.

Conclusion

1. Using MATLAB software to generate random input errors that obey the normal distribution, the kinematic reliability of the modified Delta parallel mechanism was analyzed according to the Monte Carlo method under the condition of multiple errors. At the same time, a significant amount of experimental data for statistical analysis was easily obtained using this method.
2. The reliability sensitivity of the modified Delta parallel mechanism was analyzed using the method of structuring the response surface function. Thus, the degree of influence of each error source on the kinematic reliability of the mechanism was determined.
3. The assembly position and pose errors exhibited greater effect than dimension errors on the kinematic reliability of the modified Delta parallel mechanism.

Declaration of conflicting interests

The author(s) declared no potential conflicts of interest with respect to the research, authorship, and/or publication of this article.

Funding

The author(s) disclosed receipt of the following financial support for the research, authorship, and/or publication of this article: This work was partially funded by the USTL excellent talents training foundation (China; grant no. 2015RC12).

References

1. Clavel R. Device for the movement and positioning of an element in space. Patent 4976582-ZH, USA, 1990.
2. Tsai LW. Multi-degree-of-freedom mechanism for machine tools and the like. Patent 5656905-ZH, USA, 1997.
3. Tsai LW, Walsh GC, and Stamper RE. Kinematics of novel three DOF translational platforms. In: *Proceedings of the IEEE international conference on Robotics and Automation*, Minnesota, USA, 22–28 April 1996, Part 1 (of 4), pp. 3446–3451. Minneapolis, MN: IEEE.
4. Nosova NY, Glazunov VA, Palochkin SV, et al. Synthesis of mechanisms of parallel structure with kinematic interchange. *J Machinery Manufacture Reliability* 2014; 43(5): 378–383.
5. Sun Z and Chen L. *Reliability theory and method in practical mechanism*. Beijing: Science Press, 2003, p. 11.
6. Sun Z and Zhang Y. *CNC machine tool performance and reliability design technology*. Beijing: Machinery Industry Press, 2011, p. 37.
7. Ji Y, Sun Z, and Li L. Simulation on motion reliability of crank-slider mechanism. *Acta Armanentarii* 2006; 27(1): 116–120.
8. Zhang Y. Connotation and development of mechanical reliability-based design. *J Mech Eng* 2010; 46(14): 167–185.
9. Dongyang S and Guoping C. Kinematic accuracy analysis of planar mechanisms with clearance involving random and epistemic uncertainty. *Eur J Mech A/Solids* 2016; 58: 256–261.
10. Wang D, Zhou L, Sun ZL, et al. Motion reliability analysis of ball screw pair based on Monte Carlo method. *J Northeastern Univ* 2012; 33(8): 1179–1181.
11. Guohua C, Muyuan S, Liang Y, et al. Kinematic reliability solution of 3-UPS-PU parallel mechanism based on Monte Carlo simulation. *Open Mechanical Eng J* 2015; 9(1): 324–332.
12. Xianzhen H, Sen H, Yimin Z, et al. A method to determine kinematic accuracy reliability of gear mechanisms with truncated random variables. *Mech Mach Theory* 2015; 92: 200–212.
13. Jeong K, Woo-Jin S, and Beom-Soo K. Stochastic approach to kinematic reliability of open-loop mechanism with dimensional tolerance. *Appl Math Model* 2010; 34(5): 1225–1237.
14. Wang JG, Zhang JF, and Du XP. Hybrid dimension reduction for mechanism reliability analysis with random joint clearances. *Mech Mach Theory* 2011; 46(10): 1396–1410.
15. Cui GH, Zhang HQ, Xu F, et al. Analysis of the kinematic accuracy reliability of a 3-DOF parallel robot manipulator. *Int J Adv Rob Syst* 2014; 25: 68–81.
16. Pandey MD and Zhang X. System reliability analysis of the robotic manipulator with random joint clearances. *Mech Mach Theory* 2012; 58(12): 137–152.
17. Yan M, Sun Z, and Yang Q. Analysis method of reliability sensitivity based on response surface methods. *J Mech Eng* 2007; 43(7): 67–71.
18. Pang H, Yu T, and Song B. Analyses of kinematic accuracy reliability and sensitivity for a planar linkage mechanism. *China Mech Eng* 2014; 25(18): 2415–2421.

Appendix 1

O-xyz	Global coordinate system
A_i-$x_iy_iz_i$	Reference coordinate of the fixed platform
B_i-$x_iy_iz_i$	Body-fitted coordinate system of the joints B_i
C_i-$x_iy_iz_i$	Body-fitted coordinate system of the joints C_i
D_i-$x_iy_iz_i$	Body-fitted coordinate system of the joints D_i
P-$x_iy_iz_i$	Body-fitted coordinate system of the moving platform
F_i-$x_iy_iz_i$	Reference coordinate of the moving platform
β_i	Angle measured from the x axis (O-xyz) to the xi axis (A_i-$x_iy_iz_i$)
$\boldsymbol{P}$	Position vector of the end effector
$\Delta\boldsymbol{X}$, $\boldsymbol{\theta}$	Position- and pose-error vectors of the end effector
a_i, Δa_i	Length of the driving arm (B_iC_i) and its error
c, Δc_{ij}	Length of the follower link ($C_{ij}D_{ij}$) and its error
$\boldsymbol{u}_i$	Unit vector of the driving arm
$\boldsymbol{w}_i$, $\Delta\boldsymbol{w}_i$	Unit pose vector of the follower link and its error
$e_{1ij}/2$, Δe_{1ij}	Length of the shaft C_iC_{ij} and its error
$e_{2ij}/2$, Δe_{2ij}	Length of the shaft D_iD_{ij} and its error
$\boldsymbol{r}_{1i}$, $\Delta\boldsymbol{r}_{1i}$	Configuration-position vector of the joint at point B_i and its error
$\boldsymbol{r}_{2i}$, $\Delta\boldsymbol{r}_{2i}$	Configuration-position vector of the joint at point D_i and its error
θ_{Bi}, θC_i, θ_{Di}	Pose errors of the coordinate systems B_i-$x_iy_iz_i$, C_i-$x_iy_iz_i$, D_i-$x_iy_iz_i$
${}^{O}\boldsymbol{R}_{ai}$	Transformation matrix from A_i-$x_iy_iz_i$ to O-xyz
${}^{ai}\boldsymbol{R}_{bi}$	Transformation matrix from B_i-$x_iy_iz_i$ to A_i-$x_iy_iz_i$
${}^{bi}\boldsymbol{R}_{ci}$	Transformation matrix from C_i-$x_iy_iz_i$ to B_i-$x_iy_iz_i$
${}^{O}\boldsymbol{R}_{fi}$	Transformation matrix from F_i-$x_iy_iz_i$ to O-xyz
${}^{fi}\boldsymbol{R}_{di}$	Transformation matrix from D_i-$x_iy_iz_i$ to F_i-$x_iy_iz_i$
${}^{p}\boldsymbol{R}_{fi}$	Transformation matrix from Fi-$xiyizi$ to Pi-$xiyizi$
ΔX	Position error of the end effector
Δ	Permissible error
R	Kinematic reliability of the mechanism